

The hybrid concept of turboshaft engine working according to Humphrey cycle dedicated to variety power demand – CFD analysis

ARTICLE INFO

Received: 9 November 2022
 Revised: 21 March 2023
 Accepted: 28 March 2023
 Available online: 18 May 2023

The paper presents a new concept of the turbine engine in the area of pressure gain combustion (PGE). The engine works according to Humphrey's cycle. Minor modification in construction has allowed power generation of 500 kW, 700 kW, 1000 kW, and 1800 kW. The concept successfully resolved the challenges related to the temporary opening and closing of the combustion chamber. The presented valve timing system has ensured effective gas flow and what stands behind it, an effective process of conversion of a high-pressure gas impulse into mechanical energy. Rotating combustion chambers enabled the application of an effective sealing system. The concept characterizes simple construction and potentially low power-to-weight coefficient. The CFD numerical analysis of the presented engine concept showed very promising effective efficiency and low specific fuel consumption.

Key words: *pressure gained combustion, Humphrey cycle, turbine engine, CFD analysis, valve timing system, isochoric combustion, engine energy efficiency, sealing system*

This is an open access article under the CC BY license (<http://creativecommons.org/licenses/by/4.0/>)

1. Introduction

The internal combustion engine industry is mature, but there is still a need and space for improving the performance of internal combustion engines [1, 2]. A reduction of fuel consumption, while at the same time improving power to weight ratio of the engine for existing on-market engines may be already limited. New opportunities are sought in the PGE (Pressure Gained Combustion) area [3–7].

The piston engine and classical turboshaft engine have different benefits, therefore they have found different applications. Generally, the piston engine has an advantage over the turboshaft engine in effective efficiency, while the turboshaft engine has an advantage over the piston engine in the power-to-mass ratio [7]. The paper presents the concept of a hybrid engine, as it has combined some of elements and benefits of both mentioned engines.

The fundamental assumption of the presented concept of the engine is that it has a temporary closed isochoric combustion chamber that is supplied by external compressed air. The first stage of compression is realized in the turbocharger, using the rest of the kinetic energy behind the turbine, and the second stage of compression is realized in the mechanical compressor. Secondly, a direct injection system is used. Next, the mechanical power is generated in the turbine. The concept of the engine was built to face the performance of turboshaft engines existing on the market.

Mentioned above assumption enabled the realization of the Humphrey cycle, which theoretical thermodynamic cycle has about a 10% advantage over the Bryton-Joule cycle (in compression ratio 20) [8–10]. A realization of the Humphrey cycle required the use of the valve timing system [6]. Its construction was the biggest challenge, as it had to deal with the realization of stages of the engine cycle like filling, isochoric, combustion, and exhaust. It had to ensure effective gas flow for variable thermal parameters (expansion from high to low pressure) and during the idle period [8, 12, 13]. The valve timing system has to deal with partial

turbine load. Moreover, the full tightness of the combustion chamber had to be ensured.

The paper presents the concept of a turboshaft hybrid engine for different power applications (500 kW, 700 kW, 1000 kW, and 1800 kW). The concepts differ in the volume of combustion chambers and the number of nozzles. They work at the same engine cycle parameters, using the same diameter of the turbine.

2. 500 kW power hybrid engine concept

2.1. Simulation model of the engine concept

The simulation model of the engine for 500 kW power consists of:

- six rotating combustion chambers (1300 rpm), with a single chamber volume of 0.4 dm³,
- stationary inlet of fresh air and three different de Laval nozzles in a symmetrical arrangement. The nozzles covered 2×68 degrees of turbine circumference,
- turbine with a rotational velocity of 35000 rpm and exhausted port. The turbine width was equal to 7.5 mm (Fig. 1).

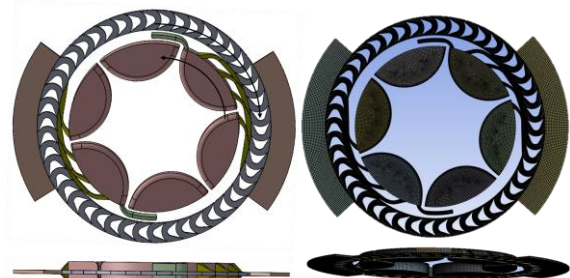


Fig. 1. Geometry model and numerical mesh—engine concept of 500 kW power

2.2. Principle of operation of the engine

Rotating combustion chambers fulfilled the role of valve timing of the engine. A single-engine cycle consists of

a filling of the combustion chamber with fresh-compressed air, direct injection of fuel, isochoric combustion, and exhaust. It was realized during 60 degrees rotation of chambers.

A pressure change for individual chambers and individual de Laval nozzles (convergent part) for 120 degrees of rotation of chambers presented is in Fig. 2. The nozzle_1 worked in the pressure range 1.7–5.0 MPa, the nozzle_2 worked in the pressure range 1.5–4.5 MPa, the nozzle_3 worked in the pressure range 1.75–3.5 MPa and the nozzle_4 worked in pressure range 1.75–2.25 MPa (Fig. 2).

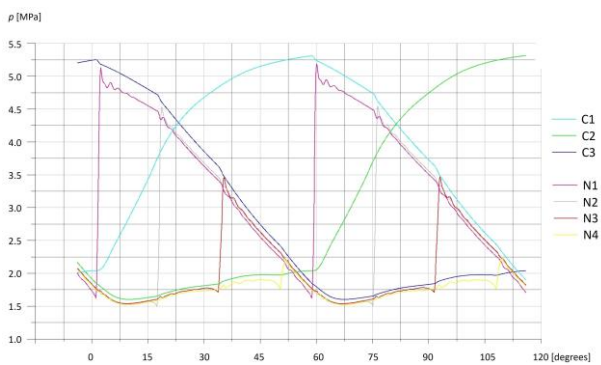


Fig. 2. Pressure change of the gas in chambers (C1, C2, C3) and nozzles (N1, N2, N3, N4) for 120 degrees rotation of chambers (2 engine cycles)

Figure 3 presents a change of oxygen content in individual combustion chambers during its 60 degrees of rotation. In chamber 1 combustion is being realized (C1-COM), in chamber 2 filling is being realized (C2-FIL) and in chamber 3 exhaust takes place (C3-EXH). Figure 4 presents the temperature distribution and Fig. 5 presents the pressure distribution at the same time of the cycle. The thermodynamic parameters pulsed according to different cycle stages. The maximum oxygen content of 18.5% was after the filling, in turn, the minimum oxygen content of 6% was after combustion. The minimum temperature of 920 K was after filling and the maximum temperature of 2320 K was after combustion. The lowest pressure of 1.6 MPa was at the beginning of filling, in turn, the maximum pressure of 5.3 MPa was at the end of combustion.

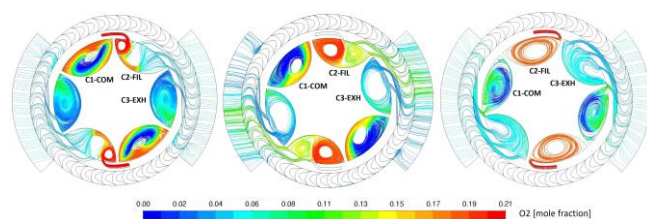


Fig. 3. Change in oxygen content of the gas for 60 degrees of rotation of chambers (1 engine cycle)

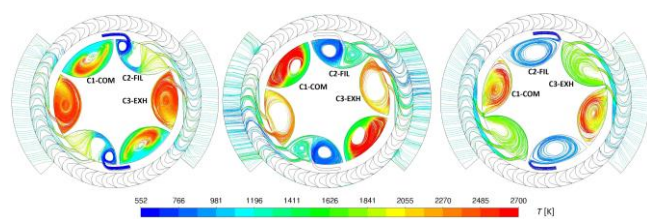


Fig. 4. Change in temperature of the gas for 60 degrees of rotation of chambers (1 engine cycle)

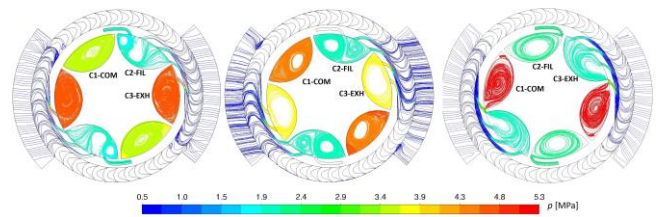


Fig. 5. Change in pressure of the gas for 60 degrees of angle rotation of chambers (1 engine cycle)

The high-pressure gas accelerated in de Laval nozzles reaching max. value of 2.8 Mach (Fig. 6).

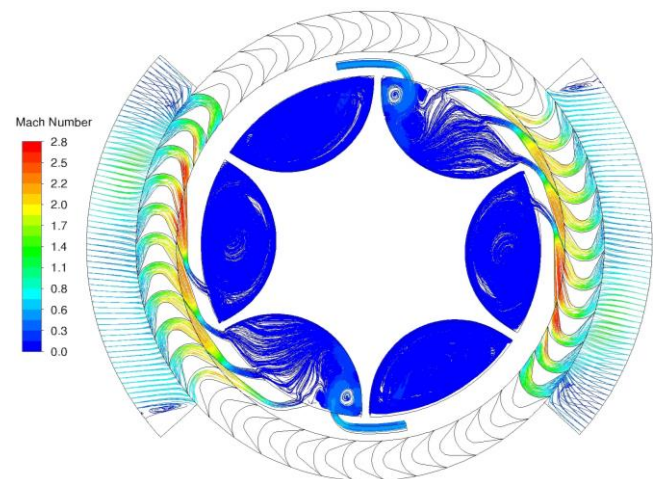


Fig. 6. The Mach number distribution

The kinetic energy of gas was transformed into mechanical energy in the turbine. Pressure distribution around the blades presented is in Fig. 7.

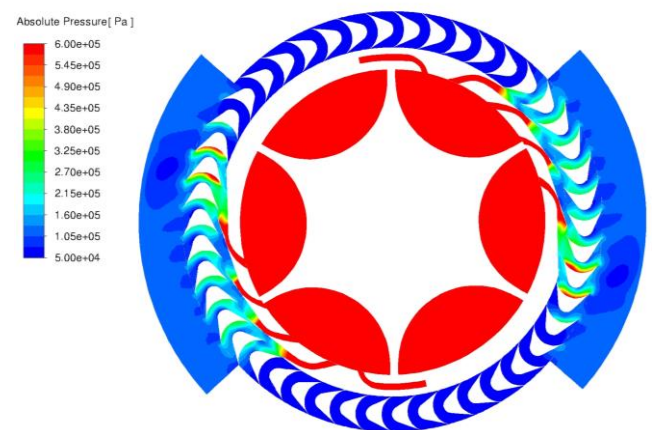


Fig. 7. The pressure distribution around the turbine blades

The torque generated in the turbine was changing from a minimum value of 60 Nm to a maximum value of 120 Nm (Fig. 8). The averaged torque was equal to 94 Nm for the symmetrical half of the engine.

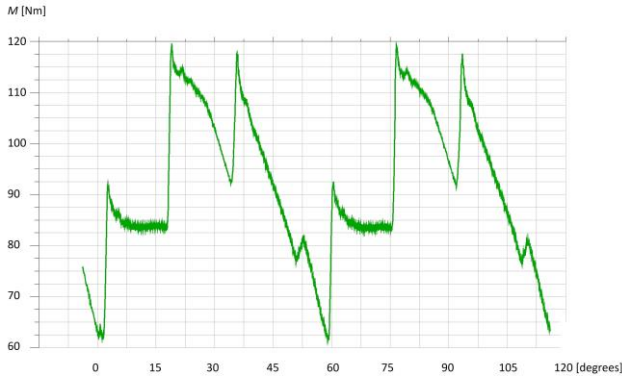


Fig. 8. Torque generated in turbine for 120 degrees rotation of chamber (2 engine cycles)

2.3. Description of the simulation approach

A transient set of Navier-Stokes equations, together with a compressible, semi-ideal, energy equation, species transport, and reaction of combustion were resolved. The thermal properties of gas species (specific heat, thermal conductivity, viscosity) were temperature-dependent. The commercial ANSYS Fluent software was employed in the analysis.

The 3D numerical simulation was performed using mesh consisting of hexahedral elements in the entire domain. The first element in the vicinity of the walls had a size of 0.25 mm. The mesh was created to assure y plus in the range of 30–300 value. The total number of elements differed from case to case between 300–600 thousand. The realizable k-ε with enhanced wall treatment option was chosen to ensure proper resolution of parameters in the boundary layer. The Rotating Mesh Motion was prescribed for rotating combustion chambers and for the turbine. The directly injected Decan was simulated using the Discrete Phase model [13]. A combustion process was simulated using the Eddy Dissipation model [15]. The excess air coefficient λ = 1.6 was assumed. The walls of the combustion chambers and walls of the nozzle were cooled. The temperature of the walls was set to 1573 K. A perfect tightness of combustion chambers was assumed. More details regarding the simulation description can be found in [15].

2.4. Evaluation of the performance of the engine concept

The 0.00012 kg of decan was injected into a single combustion chamber. The lower heat of combustion for decan was equal to 44240 kJ/kg. The 10.618 kJ of chemical energy of fuel was consumed for a single engine cycle. The kinetic energy of gas behind the turbine covered the energy demand for the turbocharger. An effective work produced by the turbine for one engine cycle (0.00769 s) was equal to 5.036 kJ. It was determined from equation (1). The mechanical efficiency of the turbine was assumed 0.95.

$$L_{eT} = \frac{M_{avg} \cdot n \cdot t_{cycle}}{9549} \eta_m \quad (1)$$

where: L_{eT} [J] – effective turbine work, M_{avg} [Nm] – averaged moment, n [rpm] – rotational velocity, t_{cycle} [s] – cycle time of discharging, $\eta_m = 0.95$ – mechanical efficiency of turbine.

The effective engine work was calculated from equation (2):

$$L_e = L_{eT} - L_{eC_mech} \quad (2)$$

where: L_e [J] – effective engine work, L_{eC_mech} [J] – effective work demand for mechanical compressor.

Using equation (3) the effective power of the engine reached 462.6 kW.

$$N_e = \frac{L_e}{t_{cycle}} \quad (3)$$

where: $L_e = L_{eT} - L_{eC_mech}$ [J] – effective engine work.

Using equation (2) the effective power of the engine reached 462.6 kW.

The engine effective efficiency reached 0.335. It was calculated from equation (4).

$$\eta_e = \frac{L_e}{E_{chem}} \quad (4)$$

where: η_e [-] – engine energy efficiency.

The specific fuel consumption was calculated from (5). It amounted to 242.9 g/kWh.

$$g = \frac{m_{C_{10}H_{22}} \cdot 1000 \cdot 3600}{t_{cycle} \cdot N_e} \quad (5)$$

where: g [g/kWh] – specific fuel consumption.

Detailed values of calculated parameters of the present engine concept presented are in Table 1.

Table 1. Calculation of performance parameters of engine concept for 500 kW power

Parameter description	Calculated value
Chemical energy of fuel	$E_{chem} = 0.00012 \text{ kg} \cdot 2 \cdot 44240 \text{ kJ/kg} = 10.618 \text{ kJ}$
Effective demand of energy for turbocharger $\eta_{eC} = \eta_{iC} \cdot \eta_T = 0.85 \cdot 0.85 \cdot 0.97 = 0.7$	$L_{eC_turboSpr} = 0.769 \text{ kJ}$
Effective demand of work for mechanical compressor $\eta_{eS} = \eta_{iS} \cdot \eta_{mS} = 0.85 \cdot 0.97 = 0.83$	$L_{eC_mech} = 1.478 \text{ kJ}$
Effective work generated by turbine	$L_{eT} = [(188 \text{ Nm} \cdot 35000 \text{ rpm} \cdot 0.00769 \text{ s}) / 9549] \cdot 0.95 = 5.036 \text{ kJ}$
The kinetic energy of gas behind the turbine	$E_{k_T} = 0.769 \text{ kJ}$
Effective work generated by engine for single engine cycle	$L_e = 5.036 - 1.478 = 3.558 \text{ kJ}$
Effective engine power	$N_e = 3.558 / 0.00769 \text{ s} = 462.6 \text{ kW}$
The effective energy efficiency of the engine	$\eta_E = 3.558 / 10.618 = 0.335$
Specific fuel consumption	$g = 0.00012 \cdot 2 \cdot 1000 \cdot 3600 / (0.00769 \cdot 462.6) = 242.9 \text{ g/kWh}$

3. 700 kW power hybrid engine concept

3.1. Simulation model of the engine concept

The simulation model of the engine for 700 kW power consists of:

- six rotating combustion chambers at 1500 rpm, with a single chamber volume of 0.5 dm³,

- stationary inlet of fresh air and three different de Laval nozzles in a symmetrical arrangement. The nozzles covered 2×51 degrees of turbine circumference,
- turbine with a rotational velocity of 35000 rpm and exhausted port. The turbine width was equal to 15 mm (Fig. 9).



Fig. 9. Geometry model and mesh of the hybrid engine concept – 700 kW power

3.2. Evaluation of the performance of the engine concept

The effective efficiency of the engine was equal to 0.351 whereas specific fuel consumption reached 232.0 g/kWh. A detailed calculation of the performance parameters of the presented engine for 700 kW power presented is in Table 2.

Table 2. Calculation of performance parameters of engine concept for 700 kW power

Parameter description	Calculated value
Chemical energy of fuel	$E_{chem} = 0.000148 \text{ kg} * 2 * 44240 \text{ kJ/kg} = 13.095 \text{ kJ}$
Effective demand of energy for turbocharger $\eta_{eC} = \eta_{iC} * \eta_T = 0.85 * 0.85 * 0.97 = 0.7$	$L_{eC_turboSpr} = 1.134 \text{ kJ}$
Effective demand of work for mechanical compressor $\eta_{eS} = \eta_{iS} * \eta_{mS} = 0.85 * 0.97 = 0.83$	$L_{eC_mech} = 1.988 \text{ kJ}$
Effective work generated by turbine	$L_{eT} = [(283.4 \text{ Nm} * 35000 \text{ rpm} * 0.00667\text{s})/9549] * 0.95 = 6.58 \text{ kJ}$
The kinetic energy of gas behind the turbine	$E_{k_T} = 1.134 \text{ kJ}$
Effective work generated by engine for single engine cycle	$L_e = 6.58 - 1.988 = 4.593 \text{ kJ}$
Effective engine power	$N_e = 4.593/0.00667 \text{ s} = 688.5 \text{ kW}$
The effective energy efficiency of the engine	$\eta_E = 4.593/13.095 = 0.351$
Specific fuel consumption	$g = 0.000148 * 2 * 1000 * 3600 / (0.00667 * 688.5) = 232.0 \text{ g/kWh}$

4. 1000 kW power hybrid engine concept

4.1. Simulation model of the engine concept

The simulation model of the engine for 1000 kW power consists of:

- six rotating combustion chambers (1300 rpm), with a single chamber volume of 0.8 dm^3 ,
- stationary inlet of fresh air and four different de Laval nozzles in a symmetrical arrangement. The nozzles covered 2×68 degrees of turbine circumference,
- turbine with a rotational velocity of 35000 rpm and exhausted port. The turbine width was equal to 15 mm (Fig. 10).

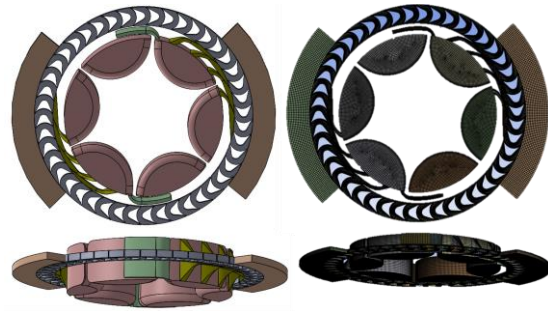


Fig. 10. Geometry model and mesh of the hybrid engine concept – 1000 kW power

4.2. Evaluation of the performance of the engine concept

The effective efficiency of the engine was equal to 0.362 whereas specific fuel consumption reached 224.6 g/kWh. A detailed calculation of the performance parameters of the presented engine for 1000 kW power presented is in Table 3.

Table 3. Calculation of performance parameters of engine concept for 1000 kW power

Parameter description	Calculated value
Chemical energy of fuel	$E_{chem} = 0.00024 \text{ kg} * 2 * 44240 \text{ kJ/kg} = 21.235 \text{ kJ}$
Effective demand of energy for turbocharger $\eta_{eC} = \eta_{iC} * \eta_T = 0.85 * 0.85 * 0.97 = 0.7$	$L_{eC_turboSpr} = 1.704 \text{ kJ}$
Effective demand of work for mechanical compressor $\eta_{eS} = \eta_{iS} * \eta_{mS} = 0.85 * 0.97 = 0.83$	$L_{eC_mech} = 2.925 \text{ kJ}$
Effective work generated by turbine	$L_{eT} = [(396.0 \text{ Nm} * 35000 \text{ rpm} * 0.00769 \text{ s})/9549] * 0.95 = 10.618 \text{ kJ}$
The kinetic energy of gas behind the turbine	$E_{k_T} = 1.704 \text{ kJ}$
Effective work generated by engine for single engine cycle	$L_e = 10.618 - 2.925 = 7.693 \text{ kJ}$
Effective engine power	$N_e = 7.693/0.00769 \text{ s} = 1000.4 \text{ kW}$
The effective energy efficiency of the engine	$\eta_E = 7.693/21.235 = 0.362$
Specific fuel consumption	$g = 0.00024 * 2 * 1000 * 3600 / (0.00769 * 1000.4) = 224.6 \text{ g/kWh}$

5. 1800 kW power hybrid engine concept – variant with 8 chambers in two rows

5.1. Simulation model of the engine concept

The simulation model of the engine for 1800 kW power consists of:

- eight rotating combustion chambers (1700 rpm), arranged in two rows with a single chamber volume of 1.8 dm^3 . Such an arrangement enabled supplying the turbine on its entire circumference.
- stationary inlet of fresh air and twelve different de Laval nozzles in a symmetrical arrangement. The nozzles covered 360 degrees of turbine circumference,
- turbine with a rotational velocity of 35000 rpm and exhausted port. The turbine width was equal to 12 mm (Fig. 11).

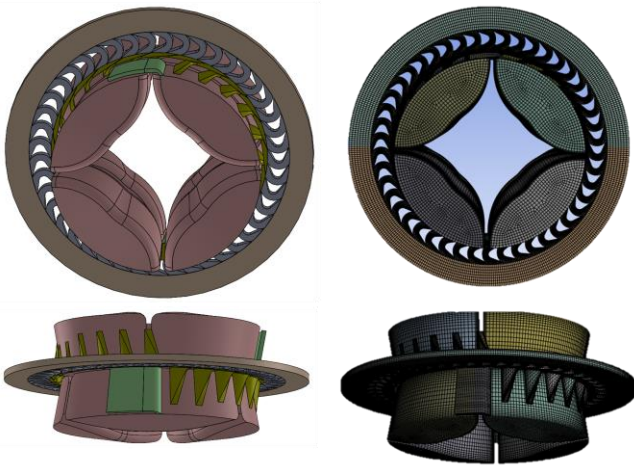


Fig. 11. Geometry model and mesh of the hybrid engine concept with 8 chambers – 1800 kW power

A pressure change for individual chambers and individual de Laval nozzles for 180 degrees of rotation of chambers presented is in Fig. 12.



Fig. 12. Pressure change of the gas in chambers (C1, C2, C3, C4) and nozzles (N1-N12) for 180 degrees rotation of chambers (2 engine cycles)

The torque generated in the turbine was changing from a minimum value of 590 Nm to a maximum value of 760 Nm (Fig. 13). The average torque was equal to 683.5 Nm.

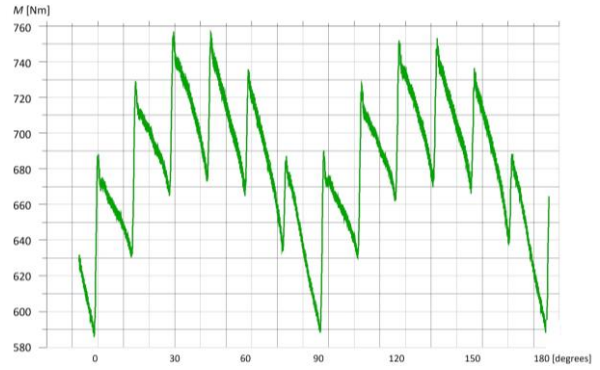


Fig. 13. Torque generated in turbine for 180 degrees rotation of chamber (2 engine cycles)

5.2. Evaluation of the performance of the engine concept

The effective efficiency of the engine was equal to 0.367 whereas specific fuel consumption reached 220.1 g/kWh. A detailed calculation of the performance parameters of the presented engine for 1800 kW power presented is in Table 4.

Table 4. Calculation of performance parameters of engine concept for 1800 kW power

Parameter description	Calculated value
Chemical energy of fuel	$E_{\text{chem}} = 0.000468 \text{ kg} * 2 * 44240 \text{ kJ/kg} = 41.746 \text{ kJ}$
Effective demand of energy for turbocharger $\eta_{\text{eC}} = \eta_{\text{ic}} * \eta_{\text{T}} = 0.85 * 0.85 * 0.97 = 0.7$	$L_{\text{eC_turbospr}} = 2.433 \text{ kJ}$
Effective demand of work for mechanical compressor $\eta_{\text{eS}} = \eta_{\text{is}} * \eta_{\text{mS}} = 0.85 * 0.97 = 0.83$	$L_{\text{eC_mech}} = 5.687 \text{ kJ}$
Effective work generated by turbine	$L_{\text{eT}} = [(683.5 \text{ Nm} * 35000 \text{ rpm} * 0.008824 \text{ s})/9549] * 0.95 = 21.000 \text{ kJ}$
The kinetic energy of gas behind the turbine	$E_{\text{k_T}} = 2.433 \text{ kJ}$
Effective work generated by engine for single engine cycle	$L_{\text{e}} = 21.000 - 5.687 = 15.313 \text{ kJ}$
Effective engine power	$N_{\text{e}} = 15.404/0.008824 \text{ s} = 1745.8 \text{ kW}$
The effective energy efficiency of the engine	$\eta_{\text{E}} = 15.313/41.746 = 0.367$
Specific fuel consumption	$g = 0.000468 * 2 * 1000 * 3600/(0.008824 * 1745.8) = 220.1 \text{ g/kWh}$

6. 1800 kW power hybrid engine concept – variant with 6 chambers in two rows

6.1. Simulation model of the engine concept

The simulation model of the engine for 1800 kW power consists of:

- six rotating combustion chambers (1700 rpm), arranged in two rows with a single chamber volume of 2.5 dm³. The such arrangement enabled supplying the turbine on its entire circumference,
- stationary inlet of fresh air and twelve different de Laval nozzles in a symmetrical arrangement. The nozzles covered 360 degrees of turbine circumference,
- turbine with a rotational velocity of 35000 rpm and exhausted port. The turbine width was equal to 12 mm (Fig. 14).



Fig. 14. Geometry model and mesh of the hybrid engine concept with 8 chambers – 1800 kW power

A pressure change for individual chambers and individual de Laval nozzles for 240 degrees of rotation of chambers presented is in (Fig. 15). Figure 16 presents a change of oxygen content in individual combustion chambers during its 60 degrees of rotation.

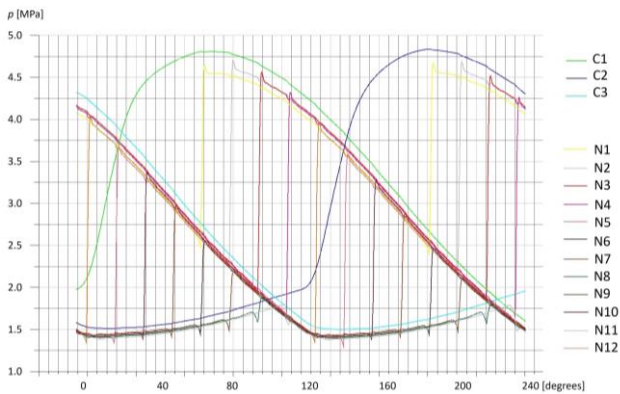


Fig. 15. Pressure change of the gas in chambers (C1, C2, C3) and nozzles (N1-N12) for 240 degrees rotation of chambers (2 engine cycles)

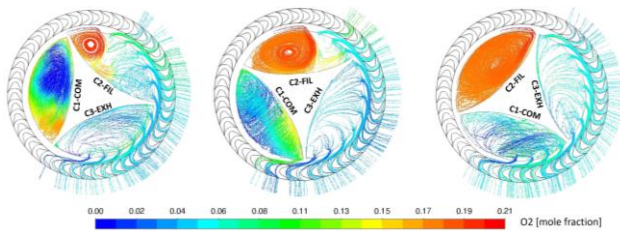


Fig. 16. Change in oxygen content of the gas for 120 degrees of rotation of chambers (1 engine cycle)

Mach distribution and pressure distribution on entire turbine circumference presented is in Fig. 17 and Fig. 18. The torque generated in the turbine was changing from a minimum value of 610 Nm to a maximum value of 750 Nm (Fig. 19). The average torque was equal to 698.0 Nm.

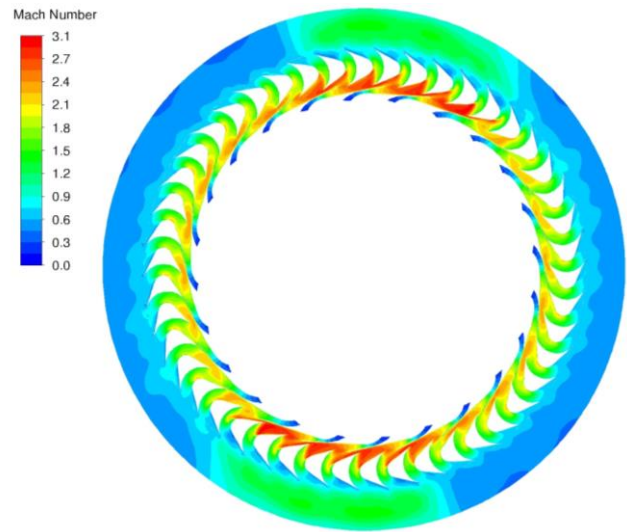


Fig. 17. Mach number distribution in nozzles and turbine

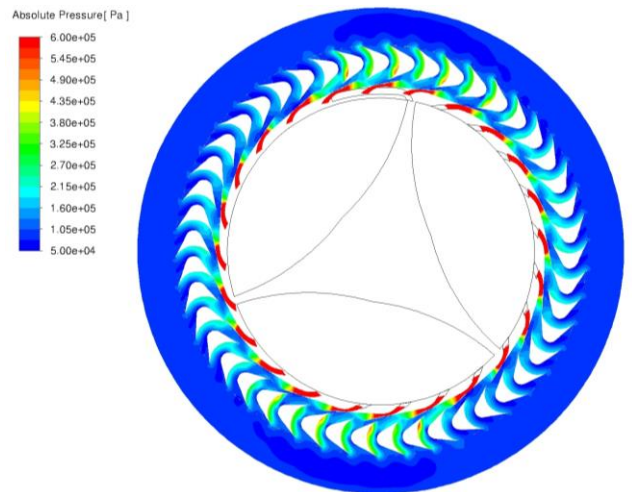


Fig. 18. Pressure distribution in nozzles and turbine

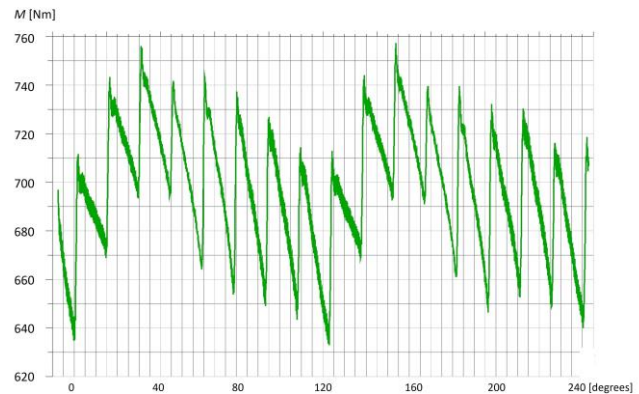


Fig. 19. Torque generated in turbine for 240 degrees rotation of chamber (2 engine cycles)

6.2. Evaluation of the performance of the engine concept

The effective efficiency of the engine was equal to 0.37 whereas specific fuel consumption reached 219.9 g/kWh (Table 5).

Table 5. Calculation of performance parameters of engine concept for 1800 kW power

Parameter description	Calculated value
Chemical energy of fuel	$E_{chem} = 0.000638 \text{ kg} * 2 * 44240 \text{ kJ/kg} = 56.467 \text{ kJ}$
Effective demand of energy for turbo-charger $\eta_{eC} = \eta_{iC} * \eta_T = 0.85 * 0.85 * 0.97 = 0.7$	$L_{eC_turbospr} = 3.285 \text{ kJ}$
Effective demand of work for me- chanical compressor $\eta_{eS} = \eta_{iS} * \eta_{mS} = 0.85 * 0.97 = 0.83$	$L_{eC_mech} = 7.697 \text{ kJ}$
Effective work generated by turbine	$L_{eT} = [(698.0 \text{ Nm} * 35000 \text{ rpm} * 0.01177 \text{ s})/9549] * 0.95 = 28.594 \text{ kJ}$
The kinetic energy of gas behind the turbine	$E_{k_T} = 3.285 \text{ kJ}$
Effective work generated by engine for single engine cycle	$L_e = 28.594 - 7.697 = 20.897 \text{ kJ}$
Effective engine power	$N_e = 20.897/0.01177 \text{ s} = 1776.2 \text{ kW}$
The effective energy efficiency of the engine	$\eta_E = 20.897/56.467 = 0.370$
Specific fuel consumption	$g = 2 * 0.000638 * 1000 * 3600/(0.01177 * 1776.2) = 219.9 \text{ g/kWh}$

combustion chamber assumption forced pulsating character of engine work. The proposed valve timing system reduced losses concerned with pulsating character to a minimum. The valve timing system aimed to come to the continuous power supply as closely as it was possible. A valve timing system ensured effective gas flow despite of idle period that appeared in the engine cycle (during combustion). It ensured continuous expansion in different de Laval nozzles and supplied the turbine on its entire circumference (for the engine concept of 1800 kW power).

A presented hybrid concept of a turboshaft engine is a promising design as it is characterized by the significant effective energy efficiency of 37.0% and low 219.9 g/kWh specific fuel consumption, with a potential small power-to-mass ratio. It has simple construction thus possibly lower production costs, compared to similar engines with isobaric combustion. It has some of the components used in piston engines like fuel injection systems and turbochargers, but there is no need for crankshaft [16]. An effective ceramic sealing system could be applied to the rotating combustion chambers. The segment sealing elements working with ceramic counter-surface can work as self-alignment because of the centrifugal force acting on them. The proposed system of seals ensures full chamber tightness, regardless of thermal conditions and related deformations.

It is worth comparing the results of the simulation to the performance parameters of turboshaft classical engines existing on the market. The hybrid engine concept has higher effective efficiency and lowers specific fuel conception for all presented power units. The highest advantage was for the smallest power (500 kW). The effective efficiency advantage was 33.5% and the percentage reduction of specific fuel consumption was 25.7% (Table 6).

The comparison however should be treated with some caution because of simulation simplification and connected with it margin error. The CFD analysis did not include thermal radiation phenomena. The simulation was done on intermediate mesh with no mesh sensitivity study. For better accuracy also more sophisticated combustion model could be required. Nevertheless, the greatest value of the research is the unique final engine concept that can efficiently realize the Humphrey cycle. It was systematically developed by studying many different constructions that are summarized in [6, 8, 12–14].

7. Conclusions

The paper presents a CFD analysis of the hybrid concept of turboshaft engine. A small modification in construction enabled its application for 500 kW, 700 kW, 1000 kW, and 1800 kW of power.

In all presented variants of the engine, the Humphrey thermodynamic cycle was realized. A temporarily closed

Table 6. Performance parameters comparison of turboshaft engines [17] and hybrid engine concept

The hybrid concept of turboshaft engine	Turboshaft engines existing on the market	Percentage advantage in efficiency	Percentage reduction of specific fuel consumption
463 kW $\eta_e = 33.5\%$, $g = 242.9 \text{ g/kWh}$	427 kW PWD207D $\eta_e = 25.1\%$, $g = 327 \text{ g/kWh}$	33.5%	25.7%
689 kW $\eta_e = 35.1\%$, $g = 232 \text{ g/kWh}$	820 kW – PT6C-67C $\eta_e = 27.5\%$, $g = 298 \text{ g/kWh}$	27.6%	22.1%
1000 kW $\eta_e = 36.2\%$, $g = 224.6 \text{ g/kWh}$	958 kW – MTR390 $\eta_e = 29.3\%$, $g = 280 \text{ g/kWh}$	23.5%	19.8%
1719 kW $\eta_e = 36.6\%$, $g = 220.1 \text{ g/kWh}$	1799 kW – RTM322 $\eta_e = 32.1\%$, $g = 255 \text{ g/kWh}$	14.0%	13.7%
1780 kW $\eta_e = 37.0\%$, $g = 219.9 \text{ g/kWh}$	1799 kW – RTM322 $\eta_e = 32.1\%$, $g = 255 \text{ g/kWh}$	15.3%	13.8%

Bibliography

- [1] Żmudka Z, Postrzednik S. Improving the effective efficiency of a spark ignition engine through the use of a fully independent valve control system. *Combustion Engines*. 2021; 187(4):30-35. <https://doi.org/10.19206/CE-141541>
- [2] Friedl H, Fraidl G, Kapus P. Highest efficiency and ultra-low emission – internal combustion engine 4.0. *Combustion Engines*. 2020;180(1):8-16. <https://doi.org/10.19206/CE-2020-102>
- [3] Brophy C, Roy G. Benefits and challenges of pressure-gain combustion systems for gas turbines. *Mech Eng*. 2009; 131(3):54-55. <https://doi.org/10.1115/1.2009-MAR-8>
- [4] Walraven F. Operational behavior of a pressure wave machine with constant volume combustion. *ABB Technical Report CHCRC 94-10*. 1994.
- [5] Kurec K, Piechna J, Gumowski K. Investigations on unsteady flow within a stationary passage of a pressure wave exchanger by means of PIV measurements and CFD calculations. *Appl Therm Eng*. 2017;112(5),610-620. <https://doi.org/10.1016/j.applthermaleng.2016.10.142>
- [6] Tarnawski P. *Konceptcja silnika turbinowego o zasilaniu pulsacyjnym*. Doctoral dissertation – Warsaw University of Technology 2018.
- [7] Kawalec M, Perkowski W, Łukasik B et al. Applications of the continuously rotating detonation to combustion engines at the Łukasiewicz – Institute of Aviation. *Combustion Engines*. 2022;191(4):51-57. <https://doi.org/10.19206/CE-145409>
- [8] Tarnawski P, Ostapski W. Pulse powered turbine engine concept – numerical analysis of influence of different valve timing concepts on thermodynamic performance. *B Pol Aca Sci-Tech*. 2018;66(3):373-382. <https://doi.org/10.24425/123444>
- [9] Tarnawski P. Analytical performance evaluation of Humphrey cycle for turbine engine application. *Machine Dynamics Research*. 2017;41(3):27-37.
- [10] Kamiuto K. Comparison of basic gas cycles under the restriction of constant heat addition. *Appl Energ*. 2006;83(6): 583-593. <https://doi.org/10.1016/j.apenergy.2005.05.008>
- [11] Stathopoulos P. Comprehensive thermodynamic analysis of the Humphrey cycle for gas turbines with pressure gain combustion. *Energies*. 2018;11(12):3521. <https://doi.org/10.3390/en11123521>
- [12] Tarnawski P, Ostapski W. Pulse powered turbine engine concept implementing rotating valve timing system – numerical CFD analysis. *J Aerospace Eng*. 2019;32(3). [https://doi.org/10.1061/\(ASCE\)AS.1943-5525.0001001](https://doi.org/10.1061/(ASCE)AS.1943-5525.0001001)
- [13] Tarnawski P, Ostapski W. A concept of a pulse-powered turbine engine with application of self-acting displacement valves-3D numerical analysis. *SAE Int J Engines*. 2021; 14(3):419-437. <https://doi.org/10.4271/03-14-03-0025>
- [14] Tarnawski P, Ostapski W. Rotating combustion chambers as a key feature of effective timing of turbine engine working according to Humphrey cycle – CFD analysis. *B Pol Aca Sci-Tech*. 2022;70(5):e143100. <https://doi.org/10.24425/bpasts.2022.143100>
- [15] *Theory Guide*. ANSYS® Academic Associate CFD, Release 16.2, Help System; ANSYS, Inc.: Canonsburg, PA, 2016.
- [16] Tikhonenkov S. An internal combustion engine without a crankshaft. *Perspectives*. *Combustion Engines*. 2020; 183(4):39-44. <https://doi.org/10.19206/CE-2020-406>
- [17] *Gas Turbine Engines*. Aviation week and space technology. <http://www.geocities.jp/nomonomo2007/AircraftDatabase/AWdata/AviationWeekPages/GTEnginesAWJan2008.pdf> (accessed on 11.11.2022).

Piotr Tarnawski, PhD – Institute of Machine Design Fundamentals, Warsaw University of Technology.
e-mail: piotr.tarnawski@pw.edu.pl

